

Determination of In-Ga-As phase diagram at 650 and LPE growth of lattice-matched In_{0.53}Ga_{0.47}As on InP

著者	中嶋 一雄
journal or publication title	Journal of Applied Physics
volume	50
number	7
page range	4975-4981
year	1979
URL	http://hdl.handle.net/10097/47314

doi: 10.1063/1.325575

Determination of In-Ga-As phase diagram at 650 °C and LPE growth of lattice-matched $\text{In}_{0.53}\text{Ga}_{0.47}\text{As}$ on InP

Kazuo Nakajima, Toshiyuki Tanahashi, Kenzo Akita, and Toyoshi Yamaoka
Fujitsu Laboratories, Ltd., 1015 Kamikodanaka, Nakahara-ku, Kawasaki, Japan

(Received 18 December 1978; accepted for publication 5 April 1979)

The liquidus isotherm in the In-rich corner of the In-Ga-As system at 650 °C was experimentally determined by an improved seed dissolution technique using InP seeds. The solidus isotherms at this temperature were also determined in the composition range close to lattice-matched $\text{In}_{0.53}\text{Ga}_{0.47}\text{As}$ on InP. The solidus data are strongly affected by the crystallographic orientation of the substrate, but are not significantly affected by the degree of lattice matching. The calculated phase diagrams have been compared with the experimental results. The conditions for equilibrium LPE growth of exactly lattice-matched ternary layers on InP (100) and (111)*B* substrates were obtained from the results of the phase diagram and lattice-constant measurements. It was found that the distribution coefficient, growth rate, and surface morphology are strongly dependent on the substrate orientation. The distribution coefficient for Ga and the growth rate at 650 °C are both larger on the (100) face than on the (111)*B* face. Hillocks often appear on the (111)*B* face irrespective of degree of lattice matching, but rarely appear on the (100) face.

PACS numbers: 81.30.Dz, 81.15.Lm, 85.30. — z

I. INTRODUCTION

The growth of lattice-matched $\text{In}_{0.53}\text{Ga}_{0.47}\text{As}$ on InP is important especially for the fabrication of infrared detectors designed for the wavelength range from 1.0 to 1.65 μm . Several reports¹⁻³ on the ternary photodiodes have been made, and many authors have reported growth conditions (i.e., melt composition, starting growth temperature, and degree of supercooling) of the ternary layers lattice matched to InP by liquid-phase epitaxy (LPE).²⁻¹⁰ Most of these growth conditions, however, were derived on the basis of the calculated phase diagram without experimental determination of the liquidus isotherm at the starting growth temperature. Therefore, it could not be known whether melts with the reported compositions were just saturated at this temperature. In order to obtain accurate LPE growth conditions, it is necessary to determine the In-Ga-As ternary phase diagram which covers the temperature and composition range permitting LPE growth under reasonable conditions. The ternary phase diagram has been experimentally investigated by various authors,¹¹⁻¹⁸ and some of them¹⁵⁻¹⁸ have reported the In-rich corner of the phase diagram. However, these results do not supply sufficient information required for the growth of lattice-matched ternary layers on InP. The experimental liquidus isotherms below 700 °C have not been reported until now. Pearsall and Hopson⁶ used the liquid observation method¹⁹ to determine the liquidus temperature concerned with growth on InP near 620 °C, but they did not report the liquidus isotherms.

For the determination of liquidus isotherms, the seed dissolution technique²⁰ can be used. In the case of the In-Ga-As system, the melt composition has generally been determined from the measured weight loss of an InAs or GaAs seed after removal of the saturated melt. When such a seed was used, however, we found that a very rough ternary polycrystalline film was always grown on it, and the melt could not be completely wiped off the surface of the seed. In order

to know the exact weight loss of the seed, the crystal film and the solidified melt must be completely separated from the seed, but they could not be taken off by chemical etching (e.g., in nitric or hydrochloric acid) without dissolving a part of the seed. Therefore, accurate liquidus data could not be obtained by using InAs or GaAs seeds.

In this investigation, the liquidus isotherm at 650 °C was experimentally determined for the first time, using an improved seed dissolution technique. In this technique, an InP seed was used as a medium for determining the As solubility in the ternary In-Ga-As melt. This liquidus data gave enough information to grow epitaxial layers on InP (100) and (111)*B* substrates using just saturated melts. The solidus isotherms at 650 °C were also determined in the composition range close to lattice-matched $\text{In}_{0.53}\text{Ga}_{0.47}\text{As}$ on InP. The results of the phase diagram and lattice-constant measurements were used to obtain the equilibrium conditions for LPE growth of the exactly lattice-matched ternary layers on the (100) and (111)*B* faces. The calculated phase diagrams using various values of the parameters reported by several authors were compared with the experimental results. Moreover, in this growth on InP, we investigated the dependence of the distribution coefficient, growth rate, and surface morphology on the crystallographic orientation of the substrate, and we also investigated whether growth from melts with a range of compositions produced the lattice-matched solid composition, as Stringfellow²¹ observed in the growth of $\text{In}_{1-x}\text{Ga}_x\text{P}$ on GaAs.

II. EXPERIMENTAL PROCEDURE AND RESULTS

A. Liquidus Isotherm

The 650 °C liquidus isotherms were determined by an improved seed dissolution technique. A ternary In + Ga + As melt was brought into contact with an InP seed at 650 °C and kept in contact at this temperature for $\frac{1}{2}$ h. If the

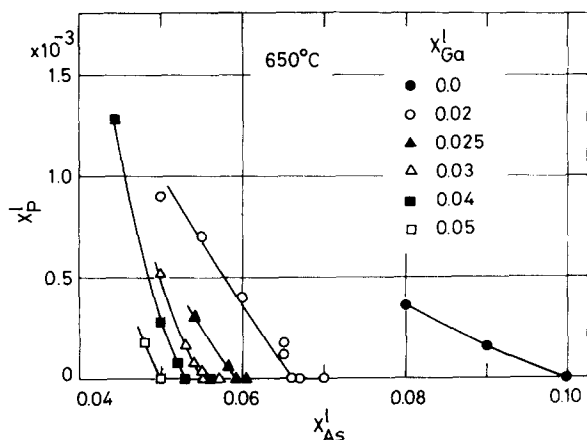


FIG. 1. P Solubility, X_P^I , at 650 °C in In-Ga-As-P quaternary melts as a function of X_{As}^I , at several values of X_{Ga}^I , as determined by the seed dissolution technique.

As concentration in the ternary melt was below the solubility limit at 650 °C, the initially undersaturated melt became saturated with P, and the P solubility could be calculated from the weight loss of the seed after removal of the melt as in the case of the In-Ga-As-P quaternary system.²² If the As concentration in the melt was just at or above the solubility limit, P could not dissolve from the InP seed, and no weight loss could be detected. P could not also be detected by an electron probe microanalyzer (EPMA) in layers grown from melts saturated with As. Therefore, the accurate ternary melt compositions just saturated at 650 °C could be known by measuring P solubility as a function of As concentration. The ternary melt was made from semiconductor-grade In, InAs, and GaAs. The InP seeds were semiconductor-grade polycrystals. The experimental apparatus consisted of a horizontal furnace system and a conventional sliding graphite boat. Pd-purified H_2 was flowed through the fused silica tube set in the furnace.

When InP seeds were used instead of InAs or GaAs ones, in most cases the quaternary or ternary solid film grew uniformly on the seed and most of the melt was removed

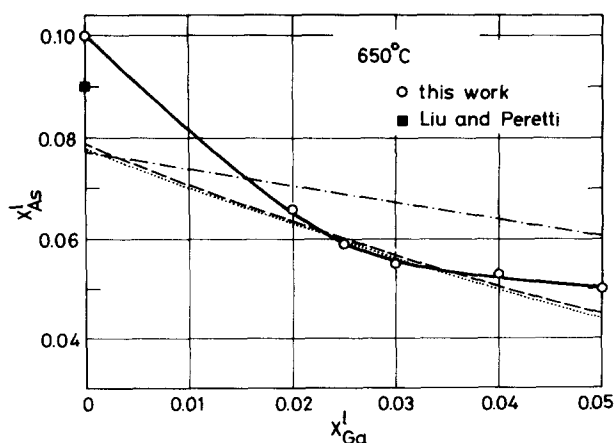


FIG. 2. Liquidus isotherm at 650 °C in the In-Ga-As ternary system, including points from this work (O) and Ref. 23 (■). Dot-dashed, broken, and dotted lines are the liquidus isotherms calculated using the parameters listed in Table II, Ref. 6, and Ref. 16, respectively.

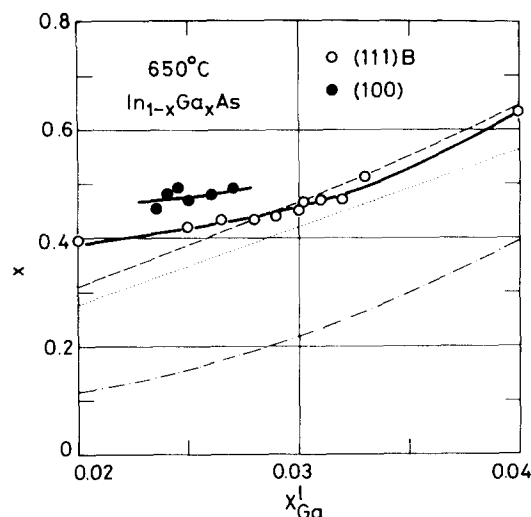


FIG. 3. Solidus isotherms at 650 °C in the In-Ga-As ternary system. Dashed, broken, and dotted lines are the solidus isotherms calculated using the parameters listed in Table II, Ref. 6, and Ref. 16, respectively.

from the surface by sliding the boat. In these cases the film and the solidified melt could be completely etched off in nitric acid without any dissolution of the InP seed, permitting accurate measurement of the weight loss. In some cases, however, the film did not grow uniformly and could not be completely taken off. When this occurred, the experimental results were rejected.

Figure 1 shows the P solubility in melts as a function of X_{As}^I at several X_{Ga}^I , where X_i^I represents the atomic fraction of an element i in the melt. At constant X_{Ga}^I , X_P^I decreases with increasing X_{As}^I . X_P^I becomes zero at a certain value of X_{As}^I , and X_P^I remains zero when X_{As}^I is above that value. The value of X_{As}^I at which X_P^I becomes zero is the As solubility in the ternary In-Ga-As melt just saturated at 650 °C. From the values shown in Fig. 1, the liquidus isotherm of 650 °C was determined as shown in Fig. 2. The In-As binary liquidus composition interpolated from the phase diagram reported by Liu and Peretti²³ is also shown in Fig. 2.

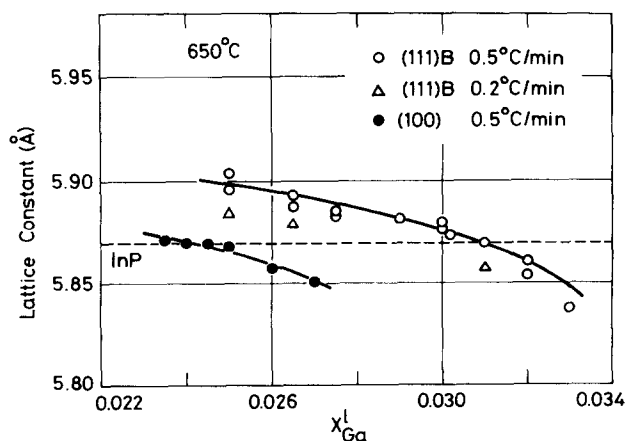


FIG. 4. Lattice constants of the $In_{1-x}Ga_xAs$ ternary alloys grown on (100) and (111)B InP substrates at 650 °C. Broken line represents the lattice constant of InP.

B. Solidus isotherms

The 650 °C solidus isotherms were determined in the vicinity of the lattice-matched solid compositions on InP. Electron microprobe analysis was performed on surfaces of $\text{In}_{1-x}\text{Ga}_x\text{As}$ epitaxial layers grown on the Sn-doped InP (100) and (111)*B* substrates. The apparatus was the same as that used for the melt saturation experiments. All the melt compositions used for the growth were determined from the liquidus isotherm shown in Fig. 2. No supersaturated melts were used. Just prior to loading, the substrates were etched in a 0.3 vol% bromine-methanol solution for several minutes. Epitaxial layers on the (111)*B* face were grown directly on the substrates. For growth on the (100) face, the substrates were cleaned by a melt-back technique using pure In for 3–5 sec immediately prior to growth of $\text{In}_{1-x}\text{Ga}_x\text{As}$. A constant cooling rate of 0.5 °C/min was used starting from an initial temperature of 650 ± 0.5 °C, and the cooling interval was between 7 and 13 °C.

EPMA, employing wavelength dispersive x-ray detection, was used to measure layer compositions. These compositions were determined from the ratios of the x-ray intensities of the Ga-*K* α and In-*L* α lines from the unknowns to those of the known stoichiometric standards GaP and InAs. Electron-beam energy was 25 keV. The measured intensities were converted to concentrations by performing the atomic number, absorption, and fluorescence corrections. Thicknesses of the layers used for EPMA were in a range from 2.5 to 4 μm .

Figure 3 shows the solidus isotherms at 650 °C. As shown in Fig. 3, the solidus data are strongly dependent on the crystallographic orientation of substrates. Therefore, there are two experimental solidus isotherms corresponding to the compositions of epitaxial layers grown on the (100) and (111)*B* substrates. The distribution coefficient of Ga in the growth of $\text{In}_{1-x}\text{Ga}_x\text{As}$ is greater on the InP (100) face than on the (111)*B* face by a factor of about 1.2. Other authors^{6,7} have also demonstrated the orientation dependence of the distribution coefficient. Our result that the distribution coefficient of Ga is larger on the (100) face is in good agreement with that reported by Pearsall *et al.*⁶

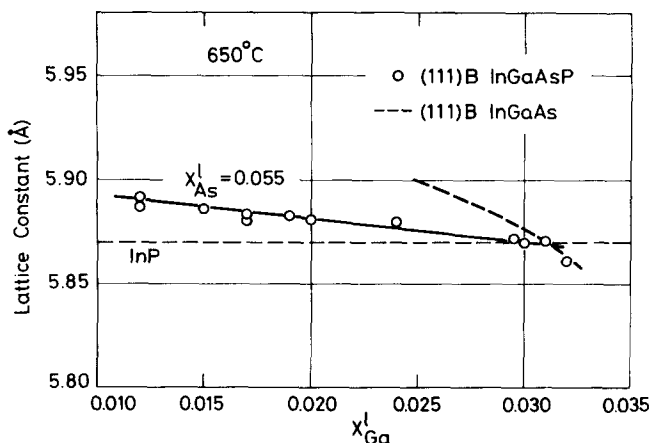


FIG. 5. Lattice constants of the $\text{In}_{1-x}\text{Ga}_x\text{As}$ and $\text{In}_{1-x}\text{Ga}_x\text{As}_{1-y}\text{P}_y$ alloys grown on InP (111)*B* substrates at 650 °C. Broken line represents the lattice constant of InP.

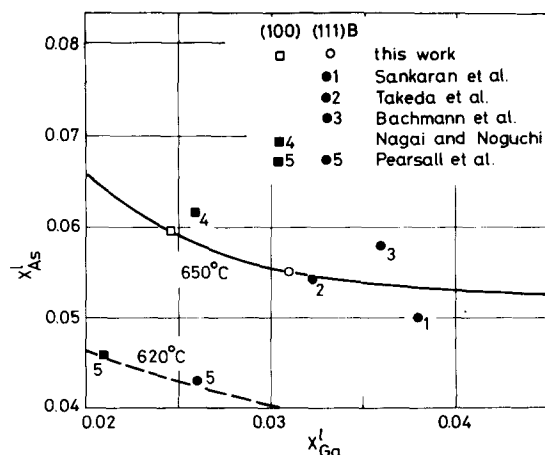


FIG. 6. Melt compositions for the growth of lattice-matched $\text{In}_{0.53}\text{Ga}_{0.47}\text{As}$ alloys on (100) and (111)*B* InP substrates. (\square and \circ) together with other authors' data from Ref. 5 (\bullet 1), Ref. 8 (\bullet 2), Ref. 2 (\bullet 3), Ref. 9 (\blacksquare 4), Ref. 6 (\bullet 5), and Ref. 10 (\blacksquare 5). The solid line is the experimentally determined liquidus isotherm at 650 °C, and the broken line is the calculated liquidus isotherm at 620 °C.

C. Equilibrium LPE growth conditions for lattice matching

The conditions for equilibrium LPE growth of lattice-matched $\text{In}_{0.53}\text{Ga}_{0.47}\text{As}$ layers on InP (100) and (111)*B* substrates were found by lattice constant measurements of these layers grown from melts with compositions on the liquidus isotherm at 650 °C. Lattice constants were measured by x-ray diffraction. The precise diffraction angles of the layers were determined from the (600) or (444) Cu-*K* β reflections by using the substrate reflection as an internal standard. The double-crystal x-ray diffraction technique was used for nearly lattice-matched samples. Samples used were grown by the ramp cooling technique described in Sec. II B.

The lattice constant is displayed as a function of X_{Ga}^I in Fig. 4. The dashed line represents the lattice constant of InP. The lattice constant of a layer grown on a (111)*B* substrate is larger than that of a layer grown on a (100) substrate from a melt with the same composition. The melt compositions required to grow lattice-matched layers on substrates with both orientations can be exactly known from these results. As also shown in Fig. 4, when the cooling rate of the LPE growth is changed from 0.5 to 0.2 °C/min, the lattice constant shifts to smaller values because the degree of composition variation with thickness of an epitaxial layer depends on cooling rate.

The dependence of lattice constants of the ternary and quaternary ($\text{In}_{1-x}\text{Ga}_x\text{As}_{1-y}\text{P}_y$) layers on melt composition is compared in Fig. 5. All of these layers were grown on (111)*B* substrates at 650 °C. The quaternary lattice constant is displayed as a function of X_{Ga}^I at $X_{\text{As}}^I = 0.055$. The emission wavelength of the lattice-matched quaternary layer at $X_{\text{As}}^I = 0.055$ is 1.62 μm at room temperature, and it is near the wavelength of the lattice-matched ternary layer, 1.65 μm . The lattice constant of ternary layers decreases more rapidly with increasing X_{Ga}^I than that of quaternary layers at $X_{\text{As}}^I = 0.055$ does.

Figure 6 shows the melt compositions for the growth of

TABLE I. Conditions for LPE growth of lattice-matched $\text{In}_{0.53}\text{Ga}_{0.47}\text{As}$ on InP .

Substrate orient.	Growth temp. (°C)	Melt compositions		X_{As}^I	$X_{\text{Ga}}^I/X_{\text{In}}^I$ ratio	Ref.
		X_{Ga}^I	X_{In}^I			
(100)	650	0.0245	0.9149	0.0596	0.027	This work
	650	0.040	7
	650	0.026	0.912	0.062	0.028	9
	621 ± 2	0.021	0.933	0.046	0.022	10
(111)B	650	0.031	0.914	0.055	0.034	This work
	650	0.049	4
	650	0.038	0.912	0.050	0.042	5
	650	0.033	0.913	0.054	0.036	8
	645	0.036	0.906	0.058	0.040	2
	617.5	0.026	0.931	0.043	0.028	6

lattice-matched ternary layers on the InP (100) and (111)B substrates together with other authors' data. These data are listed in Table I. The solid line in Fig. 6 is the experimentally determined liquidus isotherm at 650 °C as shown in Fig. 2. The melt compositions reported by Bachmann *et al.*² and by Nagai and Noguchi⁹ are slightly oversaturated at 650 °C, and the composition reported by Sankaran *et al.*⁵ is undersaturated. The data of Pearsall *et al.*⁶ at 620 °C are also shown in Fig. 6 with the 620 °C liquidus isotherm calculated using their reported parameters. Our results for lattice-matched ternary layers indicate that the distribution coefficient for Ga is 7.6 on the (111)B face and 9.6 on the (100) face, and the results also show that the distribution coefficient for As is 9.1 on the (111)B face and 8.4 on the (100) face. Other authors' data show the same tendency that the distribution coefficient for Ga is larger on the (100) face than on the (111)B face and the case for As is the reverse. Recently, Antypas *et al.*²⁴ reported the temperature dependence of the incorporation of Ga during LPE growth of lattice-matched InGaAs on InP substrates, and they stated that the distribution coefficient for Ga was higher for growth at 650 °C on (111)B substrates than on (100) substrates. However, their result is contrary to our own findings. As shown in Table I, for each orientation our value of the $X_{\text{Ga}}^I/X_{\text{In}}^I$ ratio required to grow lattice-matched layers at 650 °C is the smallest of the listed values.

D. Substrate orientation dependence of growth rate

All the layers used for measurement of thickness were grown from melts that were just saturated at the starting growth temperature, 650 °C. A constant cooling rate of 0.5 °C/min was used. These layers were not always grown from melts with the same composition, and they therefore included both lattice-matched and lattice-mismatched layers. Figure 7 shows the thickness d of the ternary and quaternary layers as a function of the temperature interval ΔT cooled from 650 °C. All the quaternary layers were grown on the (111)B face, while the ternary layers were grown on both (100) and (111)B faces. In the quaternary system, the growth rate increases slightly with increasing X_{As}^I . The data points are rather scattered because X_{Ga}^I varied from one point to another. The growth rate of ternary layers is larger than that of quaternary ones. Figure 7 also indicates the important

result that the growth rate of ternary layers is about twice as large on the (100) face as on the (111)B face. Therefore, growth on the (100) face is suitable for preparing thick layers without cooling through a long temperature interval.

E. Surface morphology

The typical surface morphology of ternary epitaxial layers grown on the (100) and (111)B faces is shown in Fig. 8. A lattice-mismatched (111)B surface generally exhibits morphology like carapace of a turtle as shown in Fig. 8(a). Layers with much larger lattice constants than that of InP could be easily grown on (111)B substrates. However, it was difficult to grow such layers with a positive lattice mismatch, $+\Delta a/a$ (where Δa is equal to the lattice constant of the alloy layer minus the lattice constant of InP , $a = 5.869 \text{ \AA}$ on (100) substrates, and most of them were grown like islands whose cross section is shown in Fig 8(b). Hillocks with $\langle 110 \rangle$ edges as shown in Fig. 8(c) often appeared on the surface of layers grown on the (111)B face irrespective of the degree of lattice matching, but hillocks were rarely observed on surface of layers grown on the (100) face. Reducing the cooling rate on the (111)B face from 0.5 to 0.1 °C/min eliminated these hillocks because formation of hillocks strongly de-

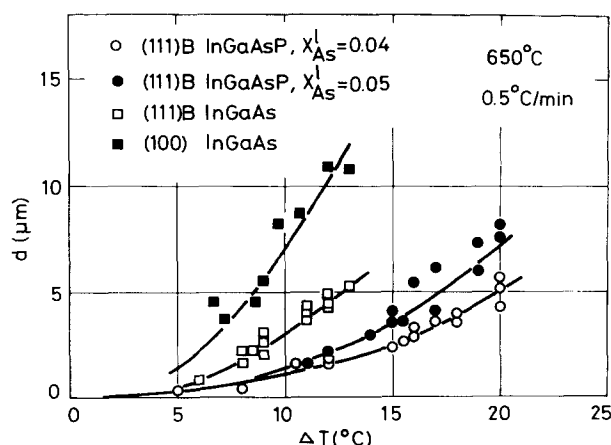
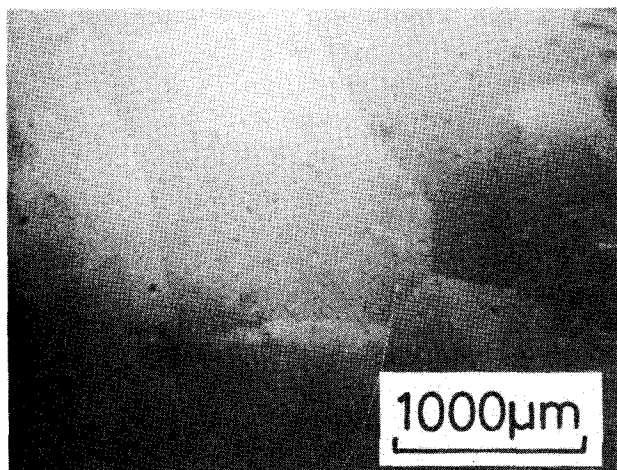
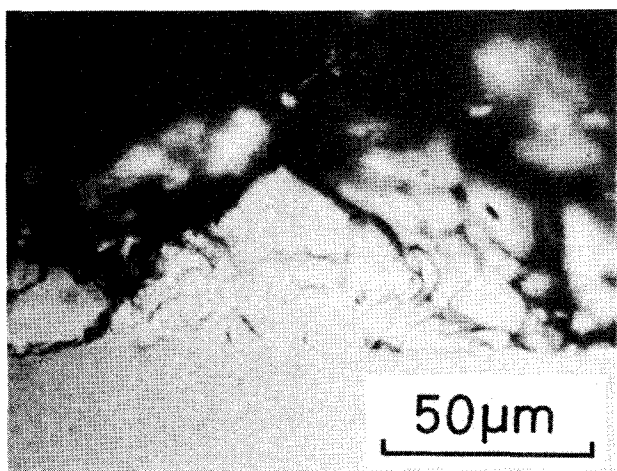


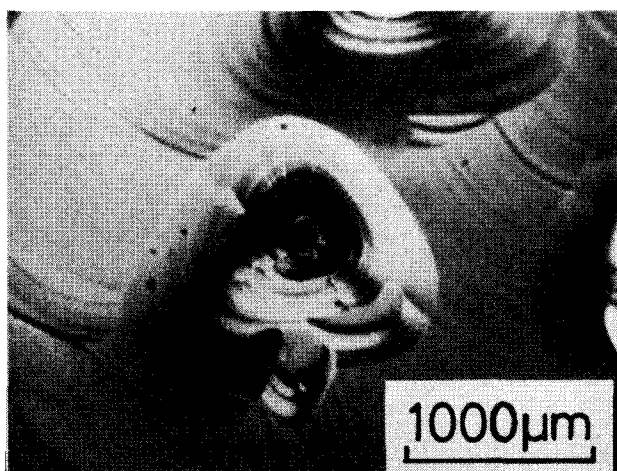
FIG. 7. Thickness d of $\text{In}_{1-x}\text{Ga}_x\text{As}$ and $\text{In}_{1-x}\text{Ga}_x\text{As}_{1-y}\text{P}_y$ layers grown on (100) and (111)B InP substrates as a function of temperature interval ΔT cooled from 650 °C.



(a)



(b)



(c)

FIG. 8. (a) Typical lattice-mismatched InGaAs surface on (111)*B* InP, with lattice misfit of +0.46%. (b) Cross section of lattice-mismatched InGaAs on (100) InP, with lattice misfit of + $\Delta a/a$. (c) Hillocks on the (111)*B* surface of InGaAs with lattice misfit of +0.08%.

depends on the depletion of Ga in front of the advancing solid-liquid interface, as reported by Sankaran *et al.*⁴ Electron microprobe analysis was performed on hillocks and the normally grown surface. It was found that hillocks contained a larger amount of Ga than the normal regions did. For exam-

ple, when the compositions of normal regions of $\text{In}_{1-x}\text{Ga}_x\text{As}$ layers were $x = 0.360$ and 0.445 , those of hillocks were $x = 0.512$ and 0.545 , respectively. Therefore, misfit dislocations appear beneath hillocks on the surface of an exactly lattice-matched layer on InP.

III. DISCUSSION

The experimentally determined isotherms have been compared with results calculated by using a simple solution model.²⁵ The parameter values in general use were adopted for the calculation. These values are listed in Table II, where T_{AB}^F and ΔS_{AB}^F are respectively the temperature and entropy of fusion of the AB compound, and Ω^l and Ω^s are the interaction parameters in the liquid and solid, respectively. The calculated liquidus isotherm at 650 °C is shown with the experimental one in Fig. 2. They are not in good agreement. One of the reasons for the disagreement is the inappropriateness of the parameters used for calculation. Most of the parameters had been derived from curve fitting with the binary or ternary experimental phase diagrams above 800 °C. Therefore, it is not surprising that the calculated results do not fit the experimental data for a temperature as low as 650 °C. To obtain reasonable agreement, values of several parameters need to be changed. Pearsall *et al.*⁶ derived new parameters Ω_{GaIn}^l (= 1850 cal/mole) and $\Omega_{\text{GaAs-InAs}}^s$ (= 2100 cal/mole) from curve fitting their experimental solidus isotherm at 620 °C. A considerable improvement in the agreement between the calculated and experimental liquidus results is achieved by using their new parameters as shown in Fig. 2. In order to obtain still better agreement, the other parameters such as Ω_{InAs}^l must be changed to better values for this temperature range. The calculated liquidus isotherm using Wu and Pearson's model¹⁶ is also shown in Fig. 2, and it is in rather good agreement with our experimental data. Their model does not present a rigorous thermodynamic treatment of solid-liquid equilibria, but it is a useful semiempirical treatment for calculating the phase diagram in this temperature range, too. The matters above mentioned suggest that the liquid solution in the In-Ga-As system is not a regular solution.

In Fig. 3 the calculated solidus isotherms are compared with our experimental results for the (100) and (111)*B* faces. The calculated result using parameters reported by Pearsall *et al.*⁶ is consistent with the experimental data for the (111)*B* face, but not with those for the (100) face. It is clear, as also pointed out by Pearsall *et al.*,¹⁰ that the effect of substrate orientation on the solidus data cannot be ignored and must be considered in the calculation of the solid composition of epitaxial layers on substrates in equilibrium with the liquid. That is to say, the energy of the free surface of the epitaxial film and the energy of adhesion of the film onto the substrate³⁰ must be added to the chemical free energy of the solid phase which is used for the calculation of the chemical equilibrium phase diagram. The surface and adhesion energies seem to be smaller on the (111)*B* face than on the (100) face because the calculated results using the chemical free energy alone are in better agreement with the experimental data for the (111)*B* face than for the (100) face.

TABLE II. Thermodynamic input data for the In-Ga-As phase diagram calculation.

$T_{\text{GaAs}}^F = 1511 \text{ K}$ (Ref. 26)	$T_{\text{InAs}}^F = 1215 \text{ K}$ (Ref. 15)
$\Delta S_{\text{GaAs}}^F = 16.64 \text{ cal/mole K}$ (Ref. 27)	$\Delta S_{\text{InAs}}^F = 14.52 \text{ cal/mole K}$ (Ref. 27)
$\Omega_{\text{GaAs}}^I = 5160 - 9.16T \text{ cal/mole}$ (Ref. 28)	$\Omega_{\text{InAs}}^I = 3860 - 10.0T \text{ cal/mole}$ (Ref. 29)
$\Omega_{\text{GaIn}}^I = 1060 \text{ cal/mole}$ (Ref. 29)	$\Omega_{\text{GaAs-InAs}}^I = 3000 \text{ cal/mole}$ (Ref. 29)

In the LPE growth of $\text{In}_{1-x}\text{Ga}_x\text{P}$ on a GaAs substrate, Stringfellow²¹ observed that growth from melts with a range of compositions produced the same solid composition, namely, the lattice-matched composition. Recently, this phenomenon was also reported in the LPE growth of $\text{In}_{1-x}\text{Ga}_x\text{As}$ on InP (111)*B* substrates.³¹ In this work, we studied whether or not this phenomenon appeared in the In-Ga-As system. The solidus isotherms in Fig. 3 show that the solid composition varies continuously with the melt composition, X_{Ga}^I , and no appreciable perturbation of the crystal composition was detected for our LPE growth conditions. Both the variation in the lattice constant versus X_{Ga}^I shown in Fig. 4 and the band gap at 300 K versus X_{Ga}^I shown in Fig. 9 support the fact that this phenomenon did not occur in the present experiments. The band-gap data plotted in Fig. 9 was determined by photoluminescence measurements which were previously reported in detail.³² When the LPE cooling rate was changed from 0.5 to 0.2 °C/min, this phenomenon did not appear either. In the calculation of the phase diagram, Stringfellow²¹ and Hirth and Stringfellow³³ suggested that the excess strain energy due to lattice mismatch must be added to the chemical free energy of the solid phase. However, we think that the surface and adhesion energy terms have more effect on the total free energy of the nearly lattice-matched epitaxial film than the strain energy terms because the solidus isotherms were much more affected by substrate orientation than by mismatching.

IV. CONCLUSIONS

The liquidus isotherm of the In-Ga-As system at 650 °C was experimentally determined by an improved seed dissolution technique using InP seeds, and the 650 °C solidus iso-

therms were determined in the composition range close to lattice-matched $\text{In}_{0.53}\text{Ga}_{0.47}\text{As}$ on InP. The calculated phase diagram using parameters derived by curve fitting the experimental phase diagram of 620 °C is in good agreement with the present experimental results. No appreciable perturbation of the crystal composition due to lattice mismatch could be detected in the LPE growth of $\text{In}_{1-x}\text{Ga}_x\text{As}$ on InP. The equilibrium conditions for the LPE growth of exactly lattice-matched ternary layers on InP (100) and (111)*B* substrates were obtained from the results of the phase diagram and lattice-constant measurements. It was found that the distribution coefficients of Ga and As, growth rate, and surface morphology are strongly dependent on the crystallographic orientation of the substrate. The distribution coefficient for Ga at 650 °C is greater on the (100) face than on the (111)*B* face by a factor of about 1.2, and the case for As is the reverse. The growth rate of the ternary layers is about twice as large on the (100) face as on the (111)*B* face, and the ternary growth rate is larger than the quaternary one in the In-Ga-As-P system. Hillocks often appear on the (111)*B* face irrespective of degree of lattice matching, but they rarely appear on the (100) face.

ACKNOWLEDGMENTS

The authors wish to acknowledge the microprobe, double-crystal x-ray, and photoluminescence measurements of T. Furusawa, Dr. S. Komiya, and A. Yamaguchi. We are grateful to Dr. O. Ryuzan, T. Kotani, and Dr. H. Takanashi for their encouragements.

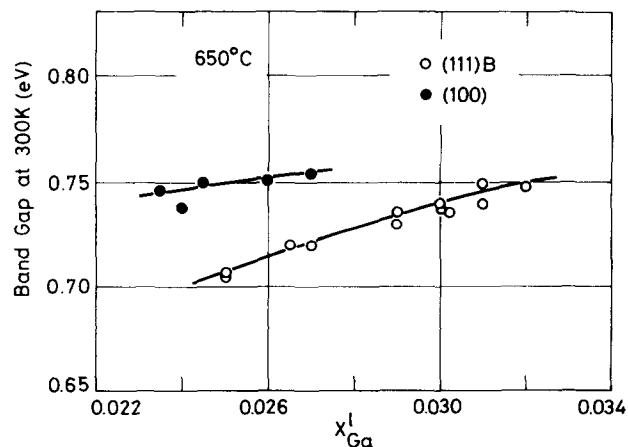


FIG. 9. Room-temperature band gaps of $\text{In}_{1-x}\text{Ga}_x\text{As}$ alloys grown on (100) and (111)*B* InP substrates as a function of X_{Ga}^I at 650 °C.

¹T.P. Pearsall and R.W. Hopson, Jr., *J. Electron. Mater.* **7**, 133 (1978).

²K.J. Bachmann and J.L. Shay, *Appl. Phys. Lett.* **32**, 446 (1978).

³T.P. Pearsall and M. Papuchon, *Appl. Phys. Lett.* **33**, 640 (1978).

⁴R. Sankaran, R.L. Moon, and G.A. Antypas, *J. Cryst. Growth* **33**, 271 (1976).

⁵R. Sankaran, G.A. Antypas, R.L. Moon, J.S. Escher, and L.W. James, *J. Vac. Sci. Technol.* **13**, 932 (1976).

⁶T.P. Pearsall and R.W. Hopson, Jr., *J. Appl. Phys.* **48**, 440 (1977).

⁷S.B. Hyder, G.A. Antypas, J.S. Escher, and P.E. Gregory, *Appl. Phys. Lett.* **31**, 551 (1977).

⁸Y. Takeda, A. Sasaki, Y. Imamura, and T. Takagi, *J. Electrochem. Soc.* **125**, 130 (1978).

⁹H. Nagai and Y. Noguchi, *Appl. Phys. Lett.* **32**, 234 (1978).

¹⁰T.P. Pearsall, R. Bisaro, R. Ansel, and P. Merenda, *Appl. Phys. Lett.* **32**, 497 (1978).

¹¹J.C. Woolley and B.A. Smith, *Proc. Phys. Soc. London* **72**, 214 (1958).

¹²H.J. Van Hook and E.S. Lenker, *Trans. Met. Soc. AIME* **227**, 220 (1963).

¹³E.F. Hockings, I. Kudman, T.E. Seidel, C.M. Schmelz, and E.F. Steigmeier, *J. Appl. Phys.* **37**, 2879 (1966).

¹⁴M.B. Panish, *J. Electrochem. Soc.* **117**, 1202 (1970).

¹⁵G.A. Antypas, *J. Electrochem. Soc.* **117**, 1393 (1970).

¹⁶T.Y. Wu and G.L. Pearson, *J. Phys. Chem. Solids* **33**, 409 (1972).

¹⁷R.E. Nahory, M.A. Pollack, and J.C. DeWinter, *J. Appl. Phys.* **46**, 775 (1975).

- ¹⁸M.A. Pollack, R.E. Nahory, L.V. Deas, and D.R. Wonsidler, *J. Electrochem. Soc.* **122**, 1551 (1975).
- ¹⁹M.B. Panish, *J. Chem. Thermodyn.* **2**, 319 (1970).
- ²⁰M. Ilegems and G.L. Pearson, in *Proc. 1968 Symposium on GaAs* (The Institute of Physics and The Physical Society, London, 1969), p. 3.
- ²¹G.B. Stringfellow, *J. Appl. Phys.* **43**, 3455 (1972).
- ²²K. Nakajima, T. Kusunoki, K. Akita, and T. Kotani, *J. Electrochem. Soc.* **125**, 123 (1978).
- ²³T.S. Liu and E.A. Peretti, *Trans. ASTM*, **45**, 677 (1953).
- ²⁴G.A. Antypas, Y.M. Houng, S.B. Hyder, J.S. Escher, and P.E. Gregory, *Appl. Phys. Lett.* **33**, 463 (1978).
- ²⁵E.A. Guggenheim, *Thermodynamics*, 5th ed. (North-Holland, Amsterdam, 1967); p. 197.
- ²⁶C.D. Thurmond, *J. Phys. Chem. Solids* **26**, 785 (1965).
- ²⁷B.D. Lichter and P. Sommelet, *Trans. AIME* **245**, 1021 (1969).
- ²⁸J.R. Arthur, *J. Phys. Chem. Solids* **28**, 2257 (1967).
- ²⁹M.B. Panish and M. Ilegems, in *Progress in Solid State Chemistry*, edited by H. Reiss and J.O. McCaldin (Pergamon, New York, 1972), Vol. 7, p. 39.
- ³⁰J.H. van der Merwe and C.A.B. Ball, in *Epitaxial Growth Part B*, edited by J.W. Matthews (Academic, New York, 1975), p. 493.
- ³¹Y. Takeda and A. Sasaki, in *Digest of 4th Int. Conf. on Vapour Growth and Epitaxy* (Nagoya, Japan, 1978), p. 197.
- ³²K. Nakajima, A. Yamaguchi, K. Akita, and T. Kotani, *J. Appl. Phys.* **49**, 5944 (1978).
- ³³J.P. Hirth and G.B. Stringfellow, *J. Appl. Phys.* **48**, 1813 (1977).